Optical NeuroImaging Instrumentation at Clarkson University

Guodong Zhang[1, 2], Charles J. Robinson[2, 3]
[1]Biomedical Engineering Program, Louisiana Tech University, Ruston LA
[2]Center for Rehabilitation Engineering, Science, and Technology, Clarkson University, Potsdam NY
[3]Research Service, Dept. of Veterans Affairs, Syracuse VA Medical Center, Syracuse, NY

Abstract

Wide-field intrinsic optical signal (IOS) imaging is used in functional cortex mapping for its excellent spatial resolution. Extrinsic dye signals can be introduced as extrinsic optical signal (EOS) imaging to improve signal noise ratio and temporal resolution. This paper describes the wide-field IOS/EOS imaging instrumentation at Clarkson University's Center for Rehabilitation Engineering, Science, and Technology (CREST). This equipment is used for neuroimaging purposes. This paper also discusses a novel method to enhance EOS through the use of self-assembled nano-particles as extrinsic dual-dye sensor preparations. Unique layer-by-layer fabrication processes are discussed, as is current research projects on sensors for *in vivo* nitric oxide imaging.

I. Introduction

The human cortex is organized into functional regions. Several imaging techniques and methods have been developed to bring higher spatial and higher temporal resolutions to functional cortical mapping. Each method has its significant advantages and limitations. Wide-field intrinsic optical signal (IOS) imaging was developed by Grinvald *et al* [2] for its excellent spatial resolution of 50-100μm [3] and non-invasive approach. Signals that can be depicted by IOS imaging include light scattering changes of neurons [4], absorption changes of hemoglobin [5], or fluorescence changes. The limitations of IOS imaging are a low signal-to-noise ratio (SNR), and a low temporal resolution since the weak intrinsic physiological signals are buried in a noisy background. It usually takes repetitive experiments between stimulated and un-stimulated states to abstract desired images out of the background, requiring a long data processing time of seconds to minutes.

To compensate for these limitations, voltage-sensitive dyes have been used as molecule transducers to transform changes in membrane potentials to fluorescence signals [3, 6]. Extrinsic Optical Signal (EOS) imaging using these extrinsic dye signals can get an improved msec temporal resolution, while still maintaining a spatial resolution of 50 to 100 μm [3]. This promising method allows real-time recording of cortical activities. These dyes are generally toxic, thereby limiting their use to acute studies.

What is required to help move the EOS field forward is a biocompatible biosensor compatible with EOS and with chronic studies, combined with good spatial resolution and temporal responsivity. Having such sensors be internally referenced would be a plus. We and others have described a nanometer-size encapsulation technique that is used to encapsulate two extrinsic dyes into one nanoparticle as a self-referenced sensor [7-9]. The technique helps control the localization of dyes and reduces or eliminates cytotoxicity. These self-referenced extrinsic fluorescence sensors signal is the ability of picturing specific desired images in have response times in milliseconds. This technique, electrostatic layer-by-layer (LbL) self-assembly, has been widely used at Louisiana Tech University to fabricate nanometer-size fluorescent dye sensors (nanosensors) [10-14].

The Electrostatic LbL self-assembly technique utilizes attractions between opposite charged polyelectrolytes to immobilize polyelectrolytes, dyes, proteins, DNAs, or charged nanometer-size particles onto templates [10, 15-17]. Nanosensors that are sensitive to pH, sodium, potassium, glucose, or oxygen have been described in several publications [1, 11, 14, 18-22]. Because of the nature of the matrix produced within the nanosensor by the LbL process, it is possible to embed firmly within that biocompatible matrix sensitive indicator dyes that are protected from starting an immunological process. Gases and small molecules can readily diffuse into this matrix, but not macrophages.

Clarkson University's recently established Center for Rehabilitation Engineering, Science and Technology (CREST) has a fully developed, high sensitivity optical neuroimaging system and a nano-biosensor fabrication lab. CREST is working in conjunction with Clarkson's Center for Advanced Materials Processing (CAMP) to bring nanotechnology into neuroscience and engineering applications. CAMP is built on Clarkson's recognized expertise in colloid and surface science and fine particle technology. It receives support from the New York State Office of Science, Technology, and Academic Research for research and operating expenses as one of 14 Centers for Advanced Technology (CATs). One thrust of CAMP is to lead a large academic/ Industry core effort in nanosystems research and development. These areas include nano-particle synthesis, nano-composites, self-assembly, and biomaterials and biological systems.

II. Instrumentation

An intrinsic optical signal (IOS) imaging system usually is consists of two main functional parts: an image capture system (e.g., camera, lens, high-speed video capture) and differential algorithms for analysis. For our fluorescent extrinsic optical signal (EOS) imaging system, a series of excitation and emission filters are required.

Some of the important properties for selecting an optimal CCD camera for an EOS imaging system are:

(i) Its full-well capacity and dynamic range, which define the maximum number of photons and the range of signal strength can be captured. The larger both of these numbers are, the better it will be to capture the signal, provided that the signal has a large dynamic range. But if the intrinsic signal is limited to an extremely low level against a high level background, a large full-well capacity will render the output images too dark. An adequate full-well capacity must fit the signal range. A larger dynamic range is always helpful in picking up the IOS imaging signals. For EOS imaging systems, the extrinsic induced signals are usually much larger than intrinsic signals and have wider signal ranges, so having a large dynamic range is a must for EOS imaging systems, as is having a higher full-well capacity to avoid saturation.

(ii) The quantum efficiency of each CCD camera indicates their sensitivity. Higher quantum efficiency can transform photons into more electron charges on CCD sensor, so both signal and noise will have a magnified magnitude. The sensitivity of CCD camera is very important so that IOS imaging systems can work with small intrinsic signals, such that very small changes in the signal can yield significant image differences in higher sensitivity cameras.

(iii) The imaging area and the resolution, which is the total surface area of the sample that can be imaged by the optics onto the CCD element of the camera, and the spatial resolution of a pixel at that magnification. The larger the image area, the better for functional neuroimaging. A larger imaging area brings more spatial information about functional neurological groups. And for spatial resolution, the average diameter of a human capillary is 8 micron. Neurons vary from 4 micron to 100 micron in diameter, so a size of a single pixel of about 10 micron would be the optimal resolution for both IOS and EOS imaging systems.

(iv) Temporal response, which is the time to capture the signal or sufficient quality to note a change in signal strength. This criterion has two components — the speed of the camera

and data acquisition software; and, the speed of the underlying physiological process being monitored. For the first, real time monitoring of perceptual quality requires a frame rate at around 30 frames per second. With that rate, it is quite difficult for the physiological systems imaged by IOS imaging to reach this speed, since the weak intrinsic signals usually require averaging over multiple frames and differential processing to reveal active areas. EOS imaging has much better temporal performance comparing to IOS imaging. Speeds in msec have been achieved with voltage-sensitive dyes (VSD). Thus, high speed functional neuroimaging (thousands of frames per second) can be achieved by high speed cameras without the sacrifice of image quality. IOS and EOS imaging systems usually use tandem lenses to maximize the imaging view, light intensity and better depth of field. The typical imaging area is around 20 mm^2, and depth of view is about several hundred microns. This limits the detection only to the surface of cortex, and to a depth of a few mm, but not deep inside the brain.

Neural Optical Imaging Setup

Figure 1 is a sketch of the EOS imaging system setup. A Xenon arc lamp generates excitation light, and this excitation is then reflected by dichromatic mirrors inside the motorized filter wheel to the tissue sample in the micro-incubator. The fluorescent nanometer-size sensors planted inside sample are then excited by this illumination light and detect oxygen or nitric oxide changes at their sites. The changes can be triggered by perfused oxygen/nitrogen air changes or perfused solutions. Electrochemical probes for oxygen or nitric oxide are probed inside micro-incubator to monitor these changes. The excited fluorescence passes through the macro lens, dichromatic mirrors and emission filters inside filter wheel, and reaches EMCCD camera. The captured images are then transferred to our computer for image processing. The images are processed in MATLAB program to subtract activity function maps and to quantify these detections.

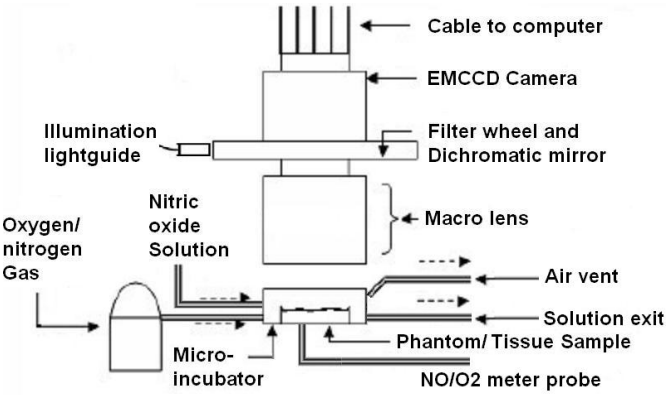

Figure 1. *Sketch of EOSI system setup*

The nanometer-sized fluorescence sensors are fabricated using electrostatic layer-by-layer (LbL) self-assembly technique. Nanofabrication on micro/nano templates relies on precise, repeatable deposition of mole-cules via self-assembly. Lvov *et al* [12, 21, 23] achieved controlled nanoconstruction by using alternating electrostatic adsorption techniques and have produced organized films that contain different polymers, proteins, and nanoparticle monolayers in precise locations directed perpendicular to the surface. The films are amorphous in a plane but are organized perpendicular to the plane with precision of a few nanometers per layer. The key aspect of this method is that a surface of almost any dimension, curvature or complexity may be covered. Thus, the films can be grown on virtually any charged substrate. This new approach of layer-by-layer assembly for building three-dimensional sub-micron structures using charged latex has been demonstrated in Figure 3. Furthermore, the potential application to biomedical problems is enhanced because biocompatible materials (e.g., chitosan, heparin, chondroitine) or hydrophilic hydrogels (e.g.,polyethylene glycol) can be used for surface modification [24, 25].

Figure 2 shows our EOS imaging system setup in detail. Fig. 2a shows the general arrangement, with the imaging camera, a stereomicroscope for specimen manipulation and operation, and a micro-incubator as the isolation chamber for samples. Fig. 2b gives a close-up of the camera and specimen chamber. In a top view, Fig. 2c shows the light source, filters and waveguides, as well as the x-axis component of the positioner. See the Figure legend for more details.

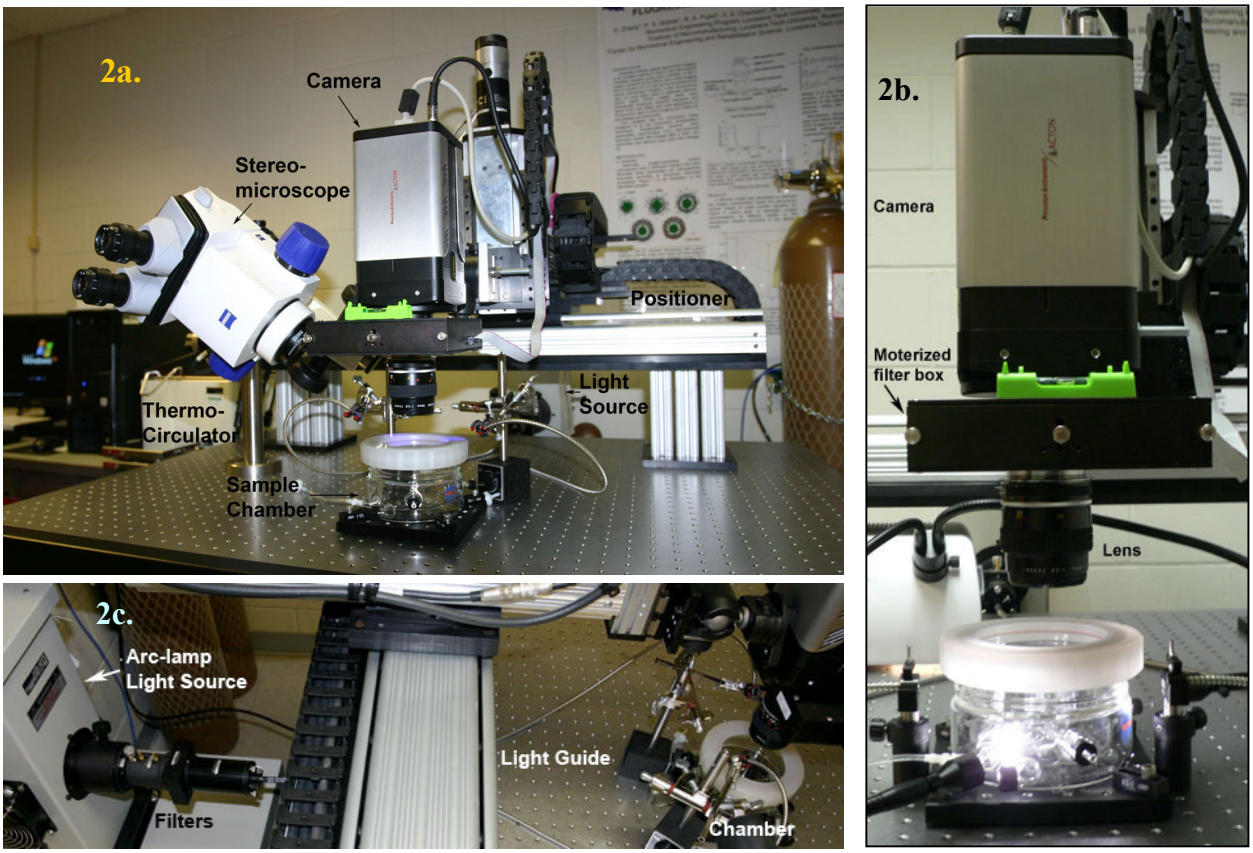

Figure 2: *These figures show the general arrangement of the Optical NeuroImaging Lab at Clarkson University.*

(a). Front view of the instrumentation on a 3" X 4' air table. In the center, the imaging camera, the Zeiss Discovery.V8 stereomicroscope for specimen manipulation and operation, and a micro-incubator as the sample isolation chamber can be seen. At the far left is the image acquisition/ analysis computer, and next to it a thermo-circulator for maintaining constant thermal environment and perfusion in the micro-incubator and its water jacket. The gas tanks on the right either are a source of variable air environment inside micro-incubator or of gas bubbled in flasks in the thermo-circulator to achieve specified partial pressures under controlled temperature conditions. The complete EOS imaging system is supported by a three-dimensional motorized positioner, which can accomplish XYZ axis movements (including focusing) and tilt/pan functions of the system.

(b). A detailed view of our EOS imaging system. The camera is a Peltier-cooled electron multiplying (EM-CCD) camera (PhotonMax 512B by Princeton Instruments). It can be cooled down to -80°C, and can multiply photon signals by 1000X. Thus, it is capable of imaging a single photon. It can also be used as a traditional CCD camera without using the multiplying function to give the camera a much higher full well capacity and dynamic range. It has >90% quantum efficiency, 512 X 512 spatial resolution, and a temporal resolution of 28 frames per second. At minimal magnification of about 1:1, this system has an imaging area of 12 X 12 mm^2 and a working distance of 100 mm. The lens currently used in this system is a Nikon macro 55 mm f/2.8 lens that can be coupled with other lenses in the future to form a tandem lens for better depth-of-field. There is a motorized filter box (Newport Corp.) between CCD camera and lens. It can contain six filters and can position each separately in the light path as directed by external TTL triggers. The filter box has been modified to allow for epi-illumination. Exchangeable dichromatic mirrors are placed inside inserts in the filter box to reflect illumination down onto the sample and to transmit the fluorescence emissions up into the camera. The key is to use a narrow band emission filter to selectively pass the spectra of interest, combined with a long-pass excitation filter to block out the much higher intensity reflected excitation frequencies. The sample chamber is a micro-incubator (Radnoti Glass Technology, Inc.). It has perfusion inlet and outlet, two sensor probe openings, and water jacket inlet and outlet. The environment inside this chamber can be precisely controlled and monitored by perfusion solution, perfusion air, and water jacket circulation for temperature control. The glass body aids optical imaging.

(c). Top view. On the left, a variable intensity Xenon arc-lamp provides the light source for the imaging system. The output of the lamp is first passed through a distilled water-based infrared filter to remove heat that would damage the following narrow-band excitation filter. The output is fed to the sample via a bifricated optical light guide. In the center is the x-axis rail and cable guide of the positioner. On the right, note the gimbaled camera mount. The light guide can also be fed into the back of the filter wheel for epi-illumination.

Assembly Technique for Nanosensors

Liquid-core micro/ nano capsules are made by depositing mutilayer thin films on weakly crosslinked particles to produce coatings of a desired thickness [1, 10-12, 14-17]. Hollow shells are formed by dissolving the core latex and getting internal diameters ranging from 20 to 10000 nm, with wall thicknesses dependent upon the number of polycation/polyanion layers (~3nm per layer). Finally, fluorescent-sensing chemistry can be loaded into the interior of the shells by a number of processes. Encouraging results have obtained in demonstrating the feasibility of using dye-encapsulating nanosensors for sensing analytes across a broad concentration range [1, 10, 11, 14]. Such mono-dispersed nano-capsules have semi-penetrable walls, with controllable permeability, and can be loaded with enzymes, fluorescent indicators, or other materials. They have been shown to be extremely stable during long-term storage and are durable when subjected to mechanical insult. This nano-technology is being pursued to produce biocompatible capsules that respond specifically to changes in sodium, potassium, calcium, pH, glucose, lactate, glutamate, nitric oxide and other moieties [1, 10, 11, 14, 21].

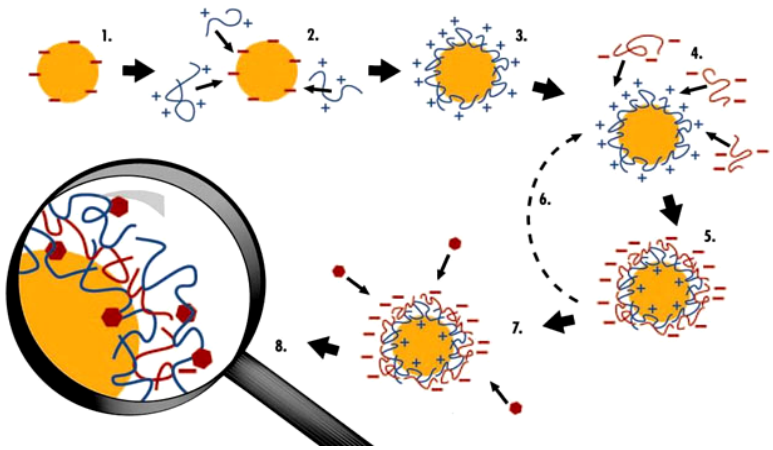

Figure 3. *Typical layer-by-layer nanosensor assembly process*
1. Negatively charged substrate; 2. Positively charged polycation adsorption; 4, 5. Negatively charged polyanion adsorption; 6. Cyclically repeat steps 3 to 5; 7. Load matrix with fluorescent indicator; 8. Rinse excess, so that all of the indicator is firmly imbedded in the matrix. [From Ref. 1].

There are several ways to load desired molecules into Layer-by-Layer self-assembled hollow capsules [17]: **(i)** Using crystals or powders of the desired molecule as the core template for layer-by-layer deposition directly. This is the simplest loading method, but the crystal or powder must be charged and stable during the whole coating process. **(ii)** Using concentration and/or potential differences to drive molecules into hollow capsules. But most of loading molecules will precipitate on the polyelectrolyte wall surface instead of staying inside the micro- or nano- capsules. **(iii)** Controlling the "opening" and "closing" of the capsule wall pores by adjusting pH value or solvent strength to trap the desired molecules inside the capsules. **(iv)** Encapsulating the desired molecules within large molecular weight polymers by diffusing monomers into the capsules and inducing polymerization afterward. The polymers will then be trapped in the capsules because of the selective permeability for small molecular weight species only.

Many other ways exist to entrap molecules within polyelectrolyte capsule walls [26]: **(i)** Replacing one polyelectrolyte species by the desired species, provided the desired molecules have similar charges of the replaced polyelectrolyte. **(ii)** Entrapping in the matrix small molecules during adsorption of charged polyelectrolytes as the small molecules are mixed into polyelectrolyte solutions and become trapped when the polyion is adsorbed. **(iii)** Pre-mixing of small molecules with polyelectrolytes, to form stable inter-molecular bonds between them. Excess charges on the polyelectrolytes allow for continued surface adsorption and multilayer formation

Using these techniques in the design of micro- and nanosensors provide possibilities of immobilization of dual dye molecules in the self-assembled capsule cores and walls. One can put the reference dye into a polymeric solution and then add a catalyst to start the polymerization. The dye will then be entrapped in the matrix. Then, using LbL techniques, a second matrix can be grown on the first and serve to house the indicator dyes.

The last consideration for any dual-labeled sensor is to ensure that the respective emission spectra do not overlap appreciably or with the excitation spectra. And the emission amplitudes should be somewhat similar, so that a proper ratio of indicator to control can be obtained. This makes the design of these dual-labeled sensors a challenge!

III. Results

Previously, we did EOS imaging of oxygen nanosensors in solution with different oxygen concentrations [8, 9]. Figure 4(a) shows the resulting oxygen nanosensor fluorescence intensity plot. A diffusion model was also developed to estimate oxygen concentration inside the solution. The estimated oxygen concentration is plotted in Figure 4(b), and the experimental result shows a very high correlation to the estimated result. The imaging of the self-assembled oxygen nanosensor using the wide-field EOS imaging technique indicates that it is feasible to use LbL self-assembled nanosensors within the EOS imaging system for accurate detection. This type of imaging concept can be used on other LbL self-assembled nanosensors.

Experimentation has started on the design of nitric oxide (NO) nanosensors. Figure 5 shows the fluorescence spectra of the self-assembled NO nanosensor containing the fluorescence dye Diaminofluorescein (DAF-2). The NO-sensitive dye DAF-2 was entrapped in crosslinked chitosan beads by ionotropic gelation. Multiple polyelectrolyte PAH/PSS bilayers were adsorbed on the surface of chitosan/DAF-2 templates to form a second matrix and to prevent the DAF-2 from leaking. The reference dye R-phycoerythrin was then loaded into this second immobilization matrix formed by the LbL self-assembled polyelectrolyte walls. The pink line in Fig. 5 is the fluorescence spectrum of chitosan/DAF-2 beads before coating them with polyelectrolyte multilayers. The blue line in Fig. 5 is the fluorescence spectrum of both the chitosan/DAF-2 cores and PAH/PSS walls in which the reference dye R-phycoerythrin is embedded. The spectroscopic measurement shows that the introduction of LbL self-assembled walls and reference dyes does not interfere the characteristics of indicator dyes. In this NO sensor design, both indicator dye DAF-2 and reference dye R-phycoerythin has an excitation wavelength at about 488nm. This saves the trouble of switching excitation filters at the light source during detection since they can be simultaneously excited. And the emission peak wavelengths of these two dyes are separated by an adequate distance, thus providing a reliable foundation for the ratiometric detection of NO based on the peak intensities of indicator and reference dyes.

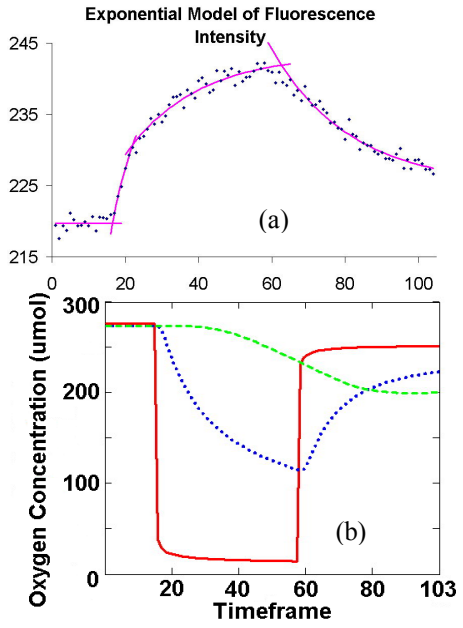

Figure 4. *Experimental results and mathematical estimates of EOS imaging of oxygen nanosensors (a) Oxygen nanosensor fluorescence intensity calculated out from EOS images. (b) Predicted oxygen concentrations in experiment solution. Red curve represents solution surface, green curve represents bottom. Blue curve represents medium layer, which has a very high correlation with EOS imaging results. This may indicate the camera was focusing at this medium layer.*

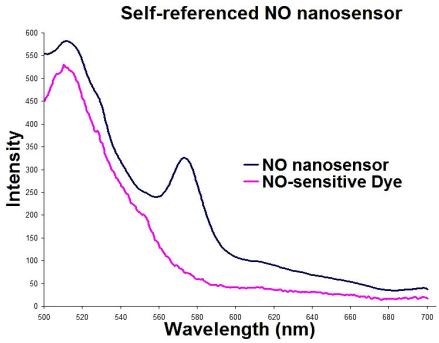

Figure 5. *Fluorescence spectra of the self-assembled NO nanosensor and the fluorescence dye Diaminofluorescein (DAF-2) used in its fabrication. Pink cure is the spectrum of chitosan/DAF-2 beads before coating polyelectrolyte multilayers. Blue curve is the spectrum of chitosan/DAF-2 core and PAH/PSS wall imbedding R-phycoerythrin.*

IV. Future Plans

The Center for Rehabilitation Engineering, Science, and Technology (CREST) at Clarkson University has been working to improve lives by combining biotechnology, clinical science, and nanoengineering. To explore to understand neurological problems such as ischemic cortical stroke, and to discover possible rehabilitation remediations, CREST established a functional neuroimaging lab with a state of the art EOS imaging system and a nanobiosensor lab that collaborates with Clarkson University's Center for Advanced Materials Processing (CAMP).

Our experiments with oxygen nanosensors helped us refine an innovative technique that can evaluate the *in situ* effects of oxygen deprivation and free-radical production on energy-sensitive ions and molecules in the intact or traumatized central nervous system, and to provide unique opportunities to relate these issues to neuronal cell dysfunction and damage and potential remediation therapies. This technique can be further applied to many other nanosensors. Currently the nanobiosensor lab has successfully fabricated NO nanosensors. The use of this NO sensor for EOS neuroimaging will be conducted in the near future with *in vitro* testing.

V. Acknowledgement

The authors would like to thank Prof. Michael McShane of Texas A&M University, Prof. Ian Suni and Prof. Shankar Subramanian of Clarkson University, and Clarkson summer REU student Jessica Berry from the Univ. of Alabama, Birmingham. Robinson is partially funded by a Senior Rehabilitation Research Career Scientist award from the US Dept of Veterans Affairs.

VI. References

[1] J. Q. Brown and M. J. McShane, "Nanoengineered polyelectrolyte micro- and nano-capsules as fluorescent potassium ion sensors," *IEEE Eng. Med. Biol. Mag.*, vol. 22, pp. 118-123, 2003.

[2] A. Grinvald, E. E. Lieke, R. D. Frostig, C. D. Gilbert, and T. N. Wiesel, "Functional architecture of cortex revealed by optical imaging of intrinsic signals," *Nature*, vol. 324, pp. 361-364, 1986.

[3] E. E. Lieke, R. D. Frostig, A. Arieli, D. Y. Ts'o, R. Hildesheim, and A. Grinvald, "Optical imaging of cortical activity: real-time imaging using extrinsic dye-signals and high resolution imaging based on slow intrinsic-signals," *Annu. Rev. Physiol.*, vol. 51, pp. 543-559, 1989.

[4] D. K. Hill and R. D. Keynes, "Opacity changes in stimulated nerve," *J. Physiol.*, vol. 108, pp. 278-281, 1949.

[5] G. A. Millikan, "Experiments on muscle hemoglobin in vivo; the instantaneous measurement of muscle metabolism," *Proc. R. Soc. B*, vol. 123, pp. 218-241, 1937.

[6] D. Shoham, D. E. Glaser, A. Arieli, T. Kenet, C. Wijnbergen, Y. Toledo, R. Hildesheim, and A. Grinvald, "Imaging cortical dynamics at high spatial and temporal resolution with novel blue voltage-sensitive dyes," *Neuron*, vol. 24, pp. 791-802, 1999.

[7] G. Zhang, M. J. McShane, and C. J. Robinson, "Using electrostatic self-assembled gradient nanosensor phantoms for calibration of an optical intrinsic signal imaging system," in *Proceedings of the 26th Annu. Int. Conf. of the IEEE-EMBS*, vol. 1. San Francisco, California, USA, 2004, pp. 1263-1266.

[8] G. Zhang, P. S. Shitole, R. A. Pujari, V. S. Charnani, M. J. McShane, and C. J. Robinson, "Intrinsic optical signal imaging of a ratiometric fluorescence oxygen nanosensor," in *Proceedings of the 3rd IEEE-EMBS Special Topic Conf. on Microtech. in Med. and Biol.* Oahu, Hawaii, USA, 2005, pp. 339-342.

[9] G. Zhang, M. J. McShane, and C. J. Robinson, "Quenching properties of a self-referenced fluorescence oxygen nanosensor under a wide-field intrinsic optical signal imaging system," in *Proceedings of the 27th Annu. Int. Conf. of the IEEE-EMBS*. Shanghai, China, 2005, pp. 1438-1441.

[10] M. J. McShane, "Nanoengineering of fluorescence-based chemical sensors using electrostatic self-assembly: thin films and micro/nanoshells," in *Proceedings of IEEE Sensors*, vol. 1. Orlando, Florida, USA, 2002, pp. 293-297.

[11] P. S. Grant and M. J. McShane, "Development of multilayer fluorescent thin film chemical sensors using electrostatic self-assembly," *IEEE Sensors J.*, vol. 3, pp. 139-146, 2003.

[12] H. Ai, S. A. Jones, and Y. M. Lvov, "Biomedical applications of electrostatic layer-by-layer nano-assembly of polymers, enzymes, and nanoparticles," *Cell Biochem. Biophys.*, vol. 39, pp. 23-43, 2003.

[13] J. Q. Brown and M. J. McShane, "Modeling of spherical fluorescent glucose microsensor systems: design of enzymatic smart tattoos," *Biosens. Bioelectron.*, vol. 21, pp. 1760-1769, 2005.
[14] K. B. Guice, M. E. Caldorera, and M. J. McShane, "Nanoscale internally referenced oxygen sensors produced from self-assembled nanofilms on fluorescent nanoparticles," *J. Biomed. Opt.*, vol. 10, pp. 64031-64041, 2005.
[15] G. Decher, "Fuzzy nanoassemblies: toward layered polymeric multicomposites," *Science*, vol. 277, pp. 1232-1237, 1997.
[16] E. Donath, G. B. Sukhorukov, F. Caruso, S. A. Davis, and H. Möhwald, "Novel hollow polymer shells by colloid-templated assembly of polyelectrolytes," *Angew. Chem. Int. Ed.*, vol. 37, pp. 2202-2205, 1998.
[17] C. S. Peyratout and L. Dähne, "Tailor-made polyelectrolyte microcapsules: from multilayers to smart containers," *Angew. Chem. Int. Ed.*, vol. 43, pp. 3762-3783, 2004.
[18] S. L. R. Barker, R. Kopelman, T. E. Meyer, and M. A. Cusanovich, "Fiber-optic nitric oxide-selective biosensors and nanosensors," *Anal. Chem.*, vol. 70, pp. 971-976, 1998.
[19] H. A. Clark, M. Hoyer, M. A. Philbert, and R. Kopelman, "Optical nanosensors for chemical analysis inside single living cells. 1. Fabrication, characterization, and methods for intracellular delivery of PEBBLE sensors," *Anal. Chem.*, vol. 71, pp. 4831-4836, 1999.
[20] H. A. Clark, R. Kopelman, R. Tjalkens, and M. A. Philbert, "Optical nanosensors for chemical analysis inside single living cells. 2. Sensors for pH and calcium and the intracellular application of PEBBLE sensors," *Anal. Chem.*, vol. 71, pp. 4837-4843, 1999.
[21] M. J. McShane, J. Q. Brown, K. B. Guice, and Y. M. Lvov, "Polyelectrolyte microshells as carriers for fluorescent sensors: loading and sensing properties of a ruthenium-based oxygen indicator," *J. Nanosci. Nanotechnol.*, vol. 2, pp. 411-416, 2002.
[22] S. M. Buck, Y.-E. L. Koo, E. J. Park, H. Xu, M. A. Philbert, M. Brasuel, and R. Kopelman, "Optochemical nanosensor PEBBLEs: photonic explorers for bioanalysis with biologically localized embedding," *Curr. Opin. Chem. Biol.*, vol. 8, pp. 540-546, 2004.
[23] H. Ai, H. Meng, I. Ichinose, S. A. Jones, D. K. Mills, Y. M. Lvov, and X. Qiao, "Biocompatibility of layer-by-layer self-assembled nanofilm on silicone rubber for neurons," *J. Neurosci. Methods*, vol. 128, pp. 1-8, 2003.
[24] H. Zhu, R. Srivastava, and M. J. McShane, "Spontaneous loading of positively charged macromolecules into alginate-templated polyelectrolyte multilayer microcapsules," *Biomacromolecules*, vol. 6, pp. 2221-2228, 2005.
[25] S. R. Nayak, K. B. Guice, Y. M. Lvov, and M. J. McShane, "Nanoengineered fluorescent sensors containing enzyme assays," in *Proceedings of the Second Joint EMBS/BMES Conference*, vol. 2. Houston, Texas, USA, 2002, pp. 1679-1680.
[26] H. Möhwald and Y. M. Lvov, *Protein Architecture: Interfacing Molecular Assemblies and Immobilization Biotechnology*: Marcel Dekker, 2000.

GUODONG ZHANG received his MS degree in Biomedical Engineering from Louisiana Tech University in Ruston, LA. He is currently pursuing his doctoral degree in the Biomedical Engineering Program at Louisiana Tech University. He is working as a Research Associate at Clarkson University's Center for Rehabilitation Engineering, Science, and Technology for his doctoral dissertation. Support for his research at Clarkson was provided by the Coulter School of Engineering.

CHARLES J. ROBINSON received his DSc degree in Electrical Engineering from Washington University in 1979. He is the founding Director of Clarkson University's Center for Rehabilitation Engineering, Science, and Technology and holds the Schulman Chair of Electrical and Computer Engineering there. He is a Senior Rehabilitation Research Career Scientist at the Syracuse VA Medical Center. He is a Fellow of the IEEE and of AIMBE.